Table 1. Effect of mutations in HIV-2 GL-AN Vpx on its expression level and viral replication ability

Results obtained in 293T cells, lymphocytic HSC-F cells, and monocyte-derived macrophage (MDM) cultures (Fujita *et al.*, 2008a, b) are summarized.

Clone	Mutation*	Vpx expression†		Viral replication‡	
		Cells	Virions	HSC-F	MDM
GL-AN	None (WT)	WT	WT	WT	WT
GL-St	ΔVpx	UD	UD	ΔVpx	UD
GL-xP103A	P103A	WT	ND	WT	WT
GL-x103/4A	P103/4A	UD	UD	M	M
GL-x106/4A	P106/4A	UD	UD	ΔVpx	UD
GL-xP109A	P109A	WT	ND	WT	M

*ΔVpx, a frame-shift mutation in the *vpx* gene (Kawamura *et al.*, 1994); see Fig. 1 for P103A, P103/4A, P106/4A and P109A mutations.
†WT, wt level expression; UD, undetectable; ND, not done. Vpx proteins in transfected 293T cells (cells) and in virions prepared from transfected 293T cells (virions) were monitored. Vpx in cells was examined by using proviral clones and/or FLAG-tagged Vpx-expression vectors.
‡WT, similar replication to wt virus; ΔVpx, similar replication to GL-St virus; UD, undetectable; M, medium replication phenotype between WT and GL-St viruses.

Although our data here on the 103/4A and 106/4A mutants were consistent with the viral growth properties (Table 1), we asked whether there is a positional effect of the FLAG tag on the Vpx expression. Expression plasmids with a C-terminal FLAG tag based on pEF1/*myc*-HisA (pEF-vpxF constructs: WT, 103/4A, 106/4A and d7P) were constructed, and their ability to express Vpx upon transfection was analysed. As shown in Fig. 1(f), the data obtained were quite similar to those in N-terminal FLAG-tagged vectors. However, the difference in the expression level between clones appeared to be smaller (Fig. 1c, f). This might result from the adjacent effect of the C-terminal FLAG tag on PPM. We used N-terminal tagged versions (pEF-Fvpx clones) thereafter.

PPM facilitates translation of Vpx in a nucleotide sequence-independent manner

The results presented so far indicated that PPM is important for Vpx expression in cells. To further understand the mechanism underlying this observation, we compared the transcription and translation efficiencies of WT and PPM mutants (Fig. 2). We firstly measured mRNA levels in cells transfected with WT or three PPM mutants (103/4A, 106/4A and d7P). Total RNA was extracted from cells and relative *vpx* mRNA level was quantified by the real-time reverse-transcription-PCR (RT-PCR) method. As shown in Fig. 2(a), mutations in PPM did not significantly change the steady-state level of each mRNA in transfected cells. In agreement with this observation, the *in vitro* transcription assay gave similar results (Fig. 2a). However, when the Vpx proteins were synthesized by an *in vitro* transcription/translation system using rabbit reticulocyte lysates, the three PPM mutants were scarcely produced (Fig. 2b). In parallel with the data obtained in transfected cells, the amount of synthesized 103/4A was confirmed to be higher than that of 106/4A in independently repeated experiments (data not shown). Furthermore, we compared the translation efficiency of WT and 106/4A clones by an *in vitro* transcription/translation system using *Escherichia coli* S30 lysates. As seen in Fig. 2(b), the PPM mutation almost abrogated the translation of Vpx even in the bacterial system.

Then, we asked whether the effect of PPM on Vpx translation is linked to the unique secondary structure and/or poly-pyrimidine tract of mRNA around the PPM-coding region (Fig. 3a). At first, mutant plasmids carrying a stop codon just upstream of PPM (G102St and +103St) were constructed (Fig. 3a), and the expression of these mutant proteins was examined in transfected cells as well as in the cell-free system using rabbit reticulocyte lysates. The truncated mutants, G102St and +103St, migrated faster than WT Vpx and were expressed at a much lower level (Fig. 3b). This was also observed in the cell-free system (Fig. 3b). These results suggested that the amino acid sequences of PPM, but not the context of the RNA sequence, are essential for efficient translation of Vpx. Moreover, we constructed various clones with synonymous mutations (106/3ccg, 106/3cca, 105ccg, 106ccg, 107ccg and 104,106ccg) that potentially disrupt the poly-pyrimidine tract (Fig. 3a), and examined their expression levels in transfected cells and in the cell-free system. As shown in Fig. 3(c), the synonymous mutants were expressed as efficiently as WT Vpx. These data also indicated that the role of Vpx PPM is primarily determined by the context of the amino acid sequences, but not by that of nucleotide sequences. Taken together (Figs 2 and 3), our findings showed that the consecutive proline residues of PPM play an essential role in efficient translation of HIV-2 Vpx both in the eukaryotic and prokaryotic systems.

PPM of HIV-2 Vpx does not have a major effect on the expression level of HIV Vpr proteins

Vpx shares many properties with Vpr including virion-association, putative three-dimensional structure, and biological activities (Fujita *et al.*, 2010). However, no PPM is present in HIV-1 and HIV-2 Vpr proteins (Khamsri *et al.*, 2006). In addition, the stoichiometry of Vpx in the virion is much higher than that of Vpr (Singh *et al.*, 2000). Approximately 4000 Vpx are estimated to be packaged in one virion, while only 14–18 HIV-1 Vpr are encapsidated. In accordance with this observation, it has been previously reported that the expression level of HIV Vpr proteins in cells is low relative to that of HIV-2 Vpx as monitored by tagged

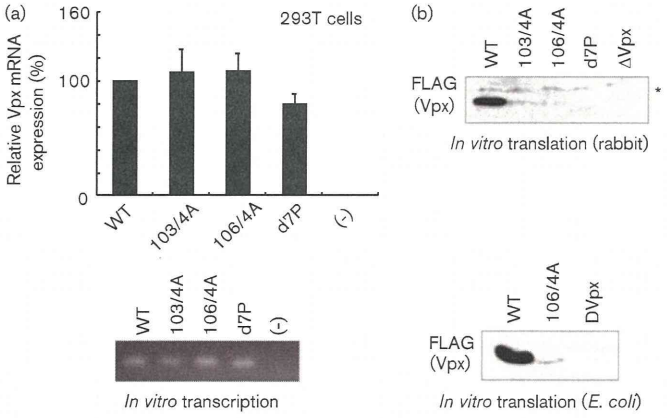

Fig. 2. Effect of PPM mutations on the expression of Vpx mRNA and protein. (a) Upper: relative amounts of Vpx mRNAs in transfected 293T cells. Total RNA was extracted from cells transfected with the expression plasmids indicated at 24 h post-transfection, and subjected to quantitative real-time RT-PCR analysis. Relative copy numbers are shown. (-), pEF1/*myc*-HisA. Lower: amounts of *in vitro* transcribed mRNAs for Vpx. (-), pEF1/*myc*-HisA. (b) Expression of Vpx–PPM mutants by an *in vitro* transcription/translation system using rabbit reticulocyte lysates (upper) or *E. coli* S30 lysates (lower). *, Non-specific bands; WT, pEF-Fvpx or pET-Fvpx; ΔVpx, pEF-FxSt or pET-FxSt.

expression plasmids/tagged proviral clones (Goujon *et al.*, 2008; Gramberg *et al.*, 2010; Khamsri *et al.*, 2006). Based on these results, we speculated that the addition of the HIV-2 Vpx PPM onto HIV-1/HIV-2 Vpr might enhance their expression.

We firstly compared expression levels of mRNA and protein for Vpx and Vpr. The mRNA levels for HIV-1 and HIV-2 Vpr proteins relative to that for HIV-2 Vpx in transiently transfected cells were measured by quantitative RT-PCR. As shown in Fig. 4(a), both Vpr mRNAs, HIV-1 Vpr in particular, were expressed to a lesser extent relative to Vpx mRNA. However, no major difference was noticed for Vpx and Vpr RNAs synthesized *in vitro* (Fig. 4a), probably due to T7 RNA polymerase in the reaction. When the protein expression levels were compared, more drastic results were obtained. HIV-1 and HIV-2 Vpr proteins were scarcely detectable in transfected cells and in the cell-free system (Fig. 4b), in contrast to Vpx. These results suggested that both transcription and translation processes are inefficient for Vpr expression. We then tested whether the PPM augments expression levels of HIV-1 and HIV-2 Vpr proteins by addition of the C-terminal flexible region of HIV-2 Vpx containing the PPM (Vpr1/Vpx and Vpr2/Vpx in Fig. 4c). In transfected cells, both Vpr1/Vpx and Vpr2/Vpx exhibited slightly higher expression relative to parental Vpr1 and Vpr2 clones, respectively (Fig. 4c). However, their expression levels obtained by adding the PPM were still much lower than that of Vpx. In addition, the *in vitro* transcription/translation analysis by rabbit reticulocyte lysates also gave little effect of the substitution with C-terminal flexible region on the translation efficiency (data not shown). These results showed that the addition of the Vpx PPM does not cause a major effect on the expression level of HIV Vpr proteins *in vivo* and *in vitro*.

SIVmac Vpx has PPM consisting of a hepta-proline stretch and its expression is PPM-dependent

For detailed analysis of Vpx and PPM-containing Vpr proteins, we generated a phylogenetic tree of various Vpx/Vpr proteins using SIVsyk (SIV from Sykes' monkeys) Vpr (without PPM) as a reference (Fig. 5). The Vpr of SIV from African green monkeys (SIVagm) has been suggested as an origin of Vpx (Sharp *et al.*, 1996). Notably, the Vpr of SIVagm clone GRI1677 has a PPM composed of five consecutive prolines, and its expression level is markedly reduced as a result of PPM-deletion (data not shown). The PPM (four consecutive prolines) of SIVmnd2 Vpx is located at a relatively similar position (106th to 109th proline) to our Vpx clone (HIV2 GL-AN in Fig. 5). Substitution mutations in this region (P106/4A) almost abolished Vpx expression (Fig. 1). Among various Vpr/Vpx proteins in Fig. 5, other than HIV-2 Vpx, Vpx proteins of SIV from drills (SIVdrl), SIVsmm and SIVmac have seven consecutive prolines.

Based on the results summarized above, we asked whether the P106/4A mutation in the Vpx–PPM of SIVmac gives an effect similar to that observed for HIV-2 Vpx (Fig. 1). As shown in Fig. 6(a), the sequence homology between the two proteins is quite high, the N-terminal half in particular, and the PPM is conserved as described above. Unexpectedly, the amount of SIVmac Vpx produced upon transfection was found to be significantly lower relative to that of HIV-2 Vpx (Fig. 6b). However, as clearly observed, the PPM mutant protein of SIVmac Vpx (106/4A) was expressed at a very reduced level relative to WT Vpx (Fig. 6b), indicating the presence of PPM-dependent regulation. We were interested in mapping the determinant(s) responsible for the different expression levels seen for HIV-2 and SIVmac Vpx proteins. Three chimeric expression plasmids were constructed, and monitored for their expression upon transfection (Fig. 6c). Since the three chimeric constructs expressed Vpx at a similarly low level to the WT SIVmac clone, the putative helix 1 in Vpx was considered to be the determinant. We substituted four amino acids in HIV-2 Vpx helix 1 with corresponding residues in the helix 1 of SIVmac Vpx (Fig. 6a, c). Expectedly, as is clear in Fig. 6(c), the mutant with the four substitutions (GL-D26N/I29V/A31E/L32I) and the WT SIVmac clone produced Vpx at a similarly low level upon

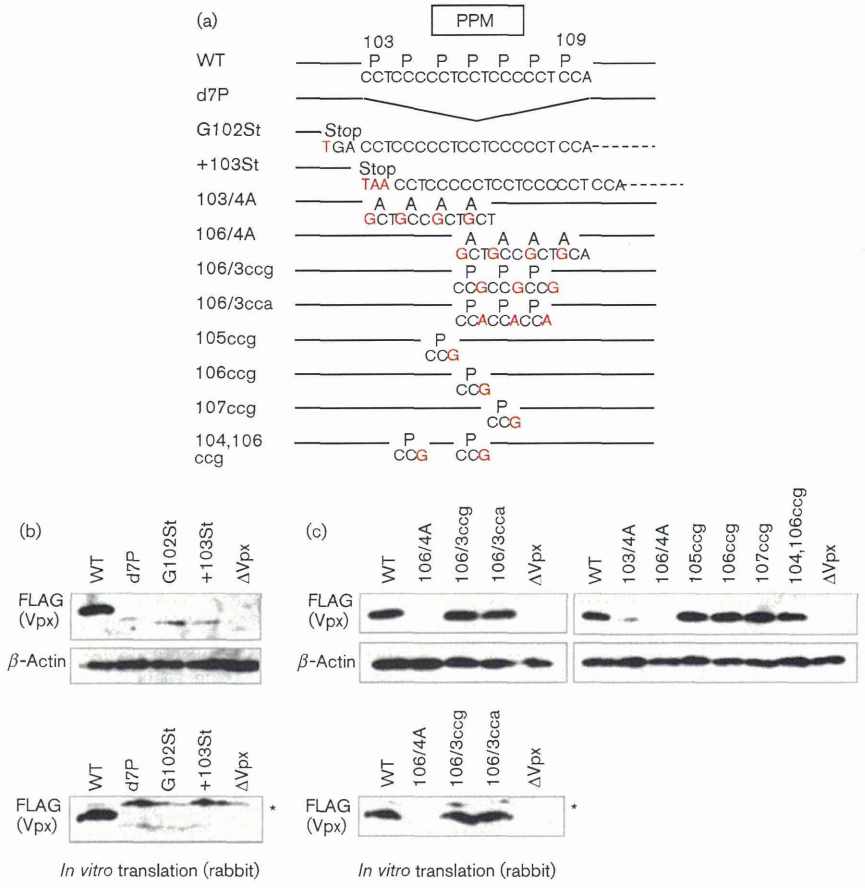

Fig. 3. Effect of poly-pyrimidine tract mutations on Vpx expression. (a) Sequences of the PPM region of WT and mutant clones. Red letters indicate nucleotides changed by mutagenesis. (b, c) Expression profiles of various Vpx–PPM mutants. Samples were prepared from transfected 293T cells (upper) or by an *in vitro* transcription/translation system using rabbit reticulocyte lysates (lower). *, Non-specific bands; WT, pEF-Fvpx; ΔVpx, pEF-FxSt.

transfection. Our results described above showed that the PPM-function itself, i.e., enhancing the Vpx expression level, is maintained in the HIV-2/SIVmac group.

DISCUSSION

One of the most prominent features for Vpx proteins of the HIV-2/SIVsmm/SIVmac group is a highly conserved PPM consisting of a hepta-proline stretch in the C-terminal region (Fig. 5). Our previous studies showed that the PPM in HIV-2 Vpx is required for Vpx expression in cells and virions (Fujita *et al.*, 2008a, b). To gain mechanistic insights into the PPM-dependent Vpx expression, we performed a systemic mutational analysis. We found that each proline residue in PPM is not equally important for Vpx expression, but that the number and position of consecutive proline residues are critical (Fig. 1). Our data showed that at least four consecutive prolines are needed to impose a clear PPM-dependency on Vpx expression. Three (or perhaps two) consecutive prolines were effective if located at the C-terminal half of PPM. Quantitative real-time RT-PCR and *in vitro* transcription/translation assays revealed that the PPM is essential for efficient translation of Vpx in both the eukaryotic and prokaryotic systems (Fig. 2). Moreover, we showed that the stretch of PPM amino acid sequence, but not the nucleotide context, is required for enhancing translation (Fig. 3).

Our data on the expression level of Vpx–PPM mutants in cells (Fig. 1) were well correlated with the ability of mutant viruses to grow in primary macrophages and lymphocytic HSC-F cells (Table 1). While mutant viruses with ability to produce Vpx at a normal level (P103A and P109A) grew comparably

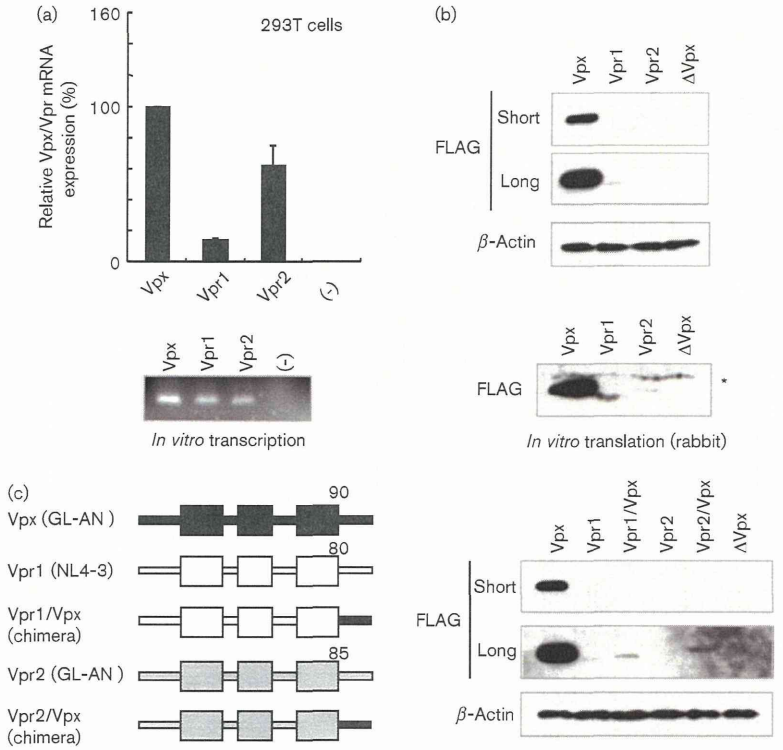

Fig. 4. Expression profiles of HIV Vpx/Vpr mRNAs and proteins. (a) Upper: expression level of Vpx/Vpr mRNAs in transfected 293T cells. Cells were transfected with the expression plasmids for HIV-2 Vpx (Vpx), HIV-1 Vpr (Vpr1) or HIV-2 Vpr (Vpr2). Total RNA was extracted at 24 h post-transfection, and subjected to quantitative real-time RT-PCR analysis with a primer set for the 3′ untranslated region of pEF1/*myc*-HisA-based vectors. Relative copy numbers are shown. (-), pEF1/*myc*-HisA. Lower: *in vitro* transcription by T7 RNA polymerase. Linearized plasmids were used as DNA templates for this assay. (-), pEF1/*myc*-HisA. (b) Upper: expression of Vpx and HIV-1/HIV-2 Vpr proteins in transfected 293T cells. Lower: expression of Vpx and HIV-1/HIV-2 Vpr proteins by an *in vitro* transcription/translation system using rabbit reticulocyte lysates. *, Non-specific bands. (c) Left: schematic structure of chimeric proteins between HIV-2 Vpx (black), HIV-1 Vpr (white), and HIV-2 Vpr (grey) proteins. Numbers indicate amino acid positions at the end of the putative third α-helix. Right: expression of Vpx/Vpr chimeric proteins in transfected 293T cells. Short, Short exposure; long, long exposure; ΔVpx, pEF-FxSt.

with parental WT virus in both cell types, a mutant (103/4A), which expresses a small amount of Vpx, grew very poorly in those cells (Fig. 1, Table 1). A mutant (106/4A), which expresses a negligible amount of Vpx, was unable to grow in macrophages and grew similarly poorly to the ΔVpx mutant virus in HSC-F cells (Fig. 1, Table 1). These results suggested that the PPM is critical for Vpx expression but not for its activity. Functionality, i.e. the potential to confer infectivity on virions, of a PPM-deletion mutant and of a Vpx/Vpr chimeric clone lacking the PPM support this conclusion (Goujon *et al.*, 2008; Gramberg *et al.*, 2010).

Very recently, it has been reported that translation elongation factor P (EF-P) is linked to the adjustment of translational efficiency for poly-proline-containing proteins in the bacterial system (Doerfel *et al.*, 2013; Ude *et al.*, 2013). During the translation, poly-proline stretch sequences tend to induce ribosome stalling, which is likely to be rescued by the EF-P (Doerfel *et al.*, 2013; Ude *et al.*, 2013). It has been reported that eIF5A, like its orthologue EF-P in the bacterial system, promotes translation of PPM-containing proteins in the yeast system (Gutierrez *et al.*, 2013). These results demonstrate the suppressive effect of poly-proline sequences on translation in cells. In contrast, our present study showed that the PPM of HIV-2 Vpx contributes to the enhancement of Vpx translation (Figs 2 and 3) and that the translational enhancement of Vpx occurs in both prokaryotic and eukaryotic machineries. How can we rationalize such opposite effects of poly-proline sequences on translation? At this moment, we do not have the answer but might assume that the HIV-2 PPM could hijack the functions of EF-P and/or eIF5A, which are the factors that stimulate the peptidyltransferase activity of the ribosome. Otherwise,

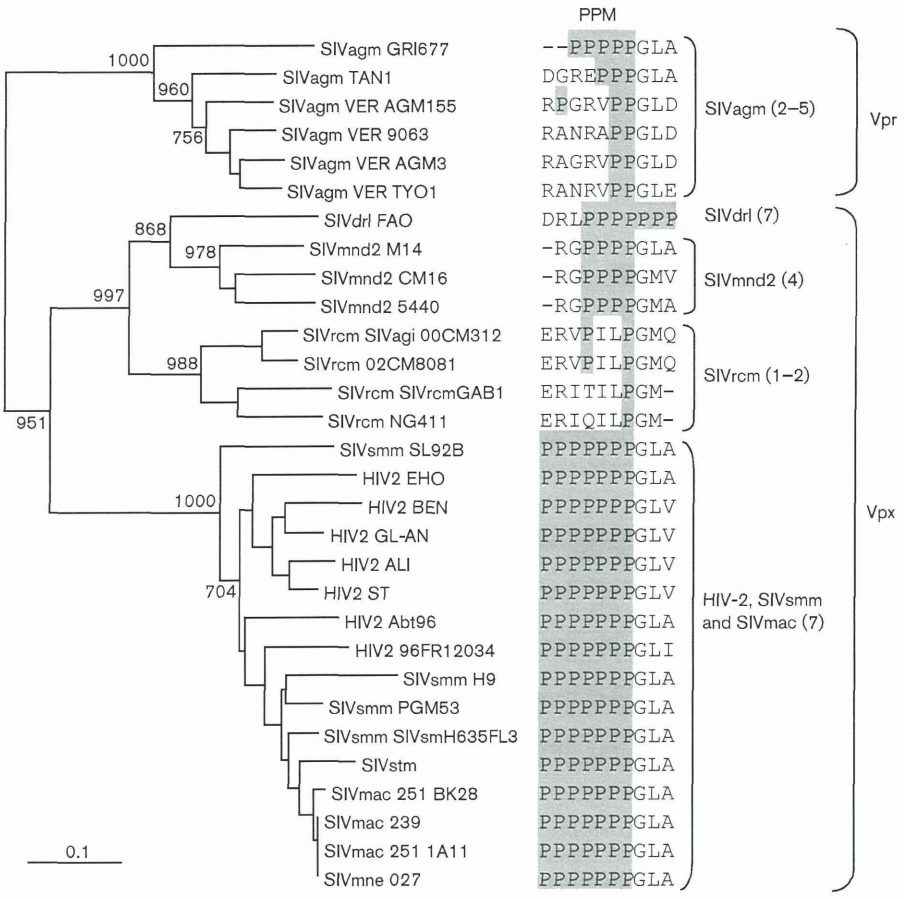

Fig. 5. Phylogenetic analysis of various Vpx and Vpr proteins. Phylogenetic tree was generated by the neighbour-joining method. The genetic distance corresponding to the lengths of branches is shown by the scale bar. Branches were calculated from 1000 bootstrap replicates, and the bootstrap values are labelled on the major branches. Amino acid sequences of the PPM region and numbers of proline residues in parentheses are shown on the right.

an additional unidentified factor(s) important for PPM-mediated protein expression may exist in cells. Moreover, of note, PPM alone did not enhance the synthesis of Vpr proteins in our present study (Fig. 4). Consistently, Vpr engineered to have the C-terminal flexible region of Vpx exhibited inefficient expression in cells, indicating that the PPM alone is insufficient for promoting protein translation (Gramberg *et al.*, 2010). There may be a region(s) and/or amino acids in Vpx other than the PPM sequence important for PPM-dependent efficient translation of Vpx. The putative helix 1 in Vpx was shown to be important for fixing its expression level in cells, but the effect of helix 1 appeared to be independent of the PPM-regulation (Fig. 6). Further study is required to elucidate the molecular mechanism for the PPM-dependent translation enhancement of Vpx.

The PPM sequence is found in a large number of prokaryotic and eukaryotic proteins (UniProt Knowledgebase, http://www.uniprot.org). As expected, a wide range of human DNA and RNA viruses encode PPM (seven or more consecutive prolines)-containing proteins. Examples include adenoviruses, herpesviruses and hepatitis viruses. However, whether these PPMs are responsible for efficient expression of the PPM-containing proteins is as yet undetermined. Extensive studies on these proteins remain to be performed to have a general picture of PPM-mediated protein expression. This paper is the first report, to the best of our knowledge, that describes and demonstrates the PPM-dependent efficient translation of animal virus proteins. Furthermore, we have shown the minimal requirements constituting a 'functional PPM' as described above (Figs 1 and 4). In HIV/SIVs, PPM sequence is also intriguing from an evolutional point of view

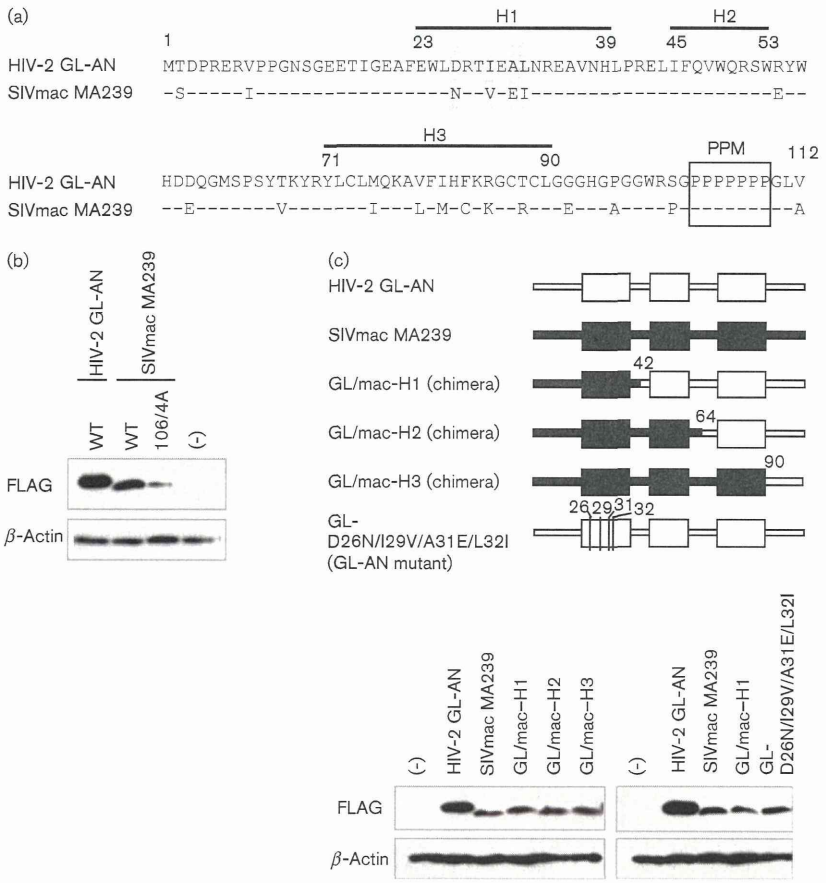

Fig. 6. Expression profiles of various SIVmac and HIV-2 Vpx proteins. (a) Sequence alignment of HIV-2 GL-AN (Kawamura *et al.*, 1994) and SIVmac MA239 (Shibata *et al.*, 1991) Vpx proteins. Numbers indicate the positions of amino acid residues in Vpx. Different amino acids in the putative first α-helix (H1) of HIV-2 GL-AN and SIVmac MA239 Vpx proteins are shaded. (b) Expression of an SIVmac Vpx–PPM mutant carrying four successive alanine substitutions at amino acids 106–109 (P106/4A) in transfected 293T cells. (c) Upper: schematic structure of chimeric proteins between HIV-2 Vpx (white) and SIVmac Vpx (black) proteins. A clone with four mutations relative to HIV-2 GL-AN Vpx is also shown. Numbers indicate the positions of amino acid residues. Lower: expression of HIV-2/SIVmac chimeric Vpx proteins and an HIV-2 mutant Vpx protein in transfected 293T cells. (-), pEF1/*myc*-HisA.

(Fig. 5). HIV-1/HIV-2 Vpr proteins without a PPM were found to be expressed at an extremely low level relative to HIV-2 Vpx (Fig. 4). While the PPM-dependent enhancement was also true for the expression of SIVmac Vpx (Fig. 6) and SIVagm Vpr (our unpublished data), some SIV Vpx/Vpr proteins lack a typical PPM sequence (three, four or more consecutive prolines) (Fig. 5). Although many of the Vpx/Vpr proteins in Fig. 5 are unanalysed to date for the function and expression, it is not unreasonable to assume that each virus in Fig. 5, during its persistent infection in its natural host, has acquired appropriate Vpx and/or Vpr for optimal viral replication and maybe for viral persistence/spread. It would be, therefore, of interest to perform functional and virological studies on the Vpx/Vpr proteins with/without PPM derived from a variety of HIV/SIVs. Studies in this direction are in progress in our laboratory.

METHODS

Plasmids. Expression plasmids for HIV-2 Vpx (GL-AN clone) (Kawamura *et al.*, 1994) with an N-terminal FLAG tag designated pME18Neo-Fvpx and its mutant derivatives have been previously described (Fujita *et al.*, 2008a, b; Khamsri *et al.*, 2006). New plasmids for various Vpx proteins with an N-terminal FLAG, pEF-F series, were constructed by introduction of an appropriate *vpx* gene fragment into pEF1/*myc*-HisA (Life Technologies). The resultant plasmids for WT and its frame-shift mutant (ΔVpx) were designated pEF-Fvpx and pEF-FxSt, respectively. Expression plasmids for HIV-1 Vpr (NL4-3 clone) (Adachi *et al.*, 1986) and HIV-2 Vpr (GL-AN),

designated pEF-Fvpr1 and pEF-Fvpr2, respectively, were constructed by replacement of the *vpx* gene in pEF-Fvpx with each *vpr* gene. Expression plasmids for Vpx/Vpr chimeras were generated by PCR-based mutagenesis using pEF-Fvpx, pEF-Fvpr1 and pEF-Fvpr2. To construct an expression plasmid for HIV-2 Vpx with a C-terminal FLAG tag, the *gag* gene of pSG-Gag cFLAG (Anraku *et al.*, 2010) was swapped with the *vpx* gene of pEF-Fvpx, and both the *vpx*-cFLAG portion and Kozak consensus sequence at the 5′ untranslated region were inserted into pEF1/*myc*-HisA (Life Technologies). The resultant plasmid was designated pEF-vpxF and used for expression of HIV-2 Vpx with a C-terminal FLAG tag. Various mutant clones were constructed from pEF-vpxF by PCR-based mutagenesis. An expression plasmid for SIVmac Vpx with an N-terminal FLAG tag was constructed by replacement of the *vpx* gene in pEF-Fvpx with SIVmac *vpx* gene (MA239 clone) (Shibata *et al.*, 1991), and designated pEF-Fvpx-SIVmac. Expression plasmids for an SIVmac Vpx mutant and HIV-2/SIVmac Vpx chimeras were generated by PCR-based mutagenesis using pEF-Fvpx and pEF-Fvpx-SIVmac. For *in vitro* transcription/translation analysis by *E. coli* S30 lysates, each *vpx* gene was inserted into pET-21b(+) (Novagen) to express Vpx with a FLAG tag at the N terminus (designated pET-Fvpx, pET-Fx106/4A, and pET-FxSt).

Transfection. Human 293T cells (Lebkowski *et al.*, 1985) were maintained in MEM medium containing 10 % heat-inactivated FBS and used for transfection experiments. For transfection, 2.5 μg of each expression plasmid DNA was introduced into 293T cells by the calcium-phosphate coprecipitation method (Adachi *et al.*, 1986). Cells were harvested at 24 h post-transfection for Western blot and RT-PCR analyses.

Western blotting. Western blot analysis was performed as described previously (Fujita *et al.*, 2008a, b). Cells were lysed in buffer composed of 10 mM Tris/HCl (pH 7.5), 10 mM NaCl, 1 % NP-40 and 1 % protease inhibitor cocktail (Sigma). Lysates were centrifuged for 5 min at 12 000 r.p.m. at 4 °C and the supernatants were used as samples after normalization of total protein amounts by a DC protein assay (Bio-Rad). Samples were separated on 12.5 or 15 % SDS-PAGE and transferred onto PVDF membranes (Immobilon-P; Millipore). The membranes were probed with anti-FLAG M2 antibody (Sigma) or anti-β-actin AC-15 antibody (Sigma), and with HRP-conjugated secondary antibody. Immunoreactive proteins were visualized by chemiluminescence using ECL Plus Western blotting detection reagents (GE Healthcare Bio-Sciences). Experiments were repeated at least three times, and the representative results are shown.

***In vitro* RNA transcription.** *In vitro* transcription was conducted by T7 RNA polymerase (New England Biolabs) using linearized plasmid DNAs (cut with *Xba*I) as templates. Transcribed RNA was quenched by EDTA and denatured by incubating at 65 °C for 15 min in MOPS, 50 % formamide and 12 % formaldehyde as indicated in the manufacturer's instructions. Denatured RNA was then mixed with ethidium bromide, separated by 1.5 % agarose gel containing MOPS and 18 % formaldehyde, and visualized by ethidium bromide staining. Experiments were repeated three times, and the representative results are shown.

***In vitro* transcription/translation.** A TNT T7 Quick Coupled Transcription/Translation System using rabbit reticulocyte lysates and a S30 T7 High-Yield Protein Expression System (Promega) were used to monitor the Vpx/Vpr expression in eukaryotic and prokaryotic cell-free systems, respectively. *In vitro* reactions were conducted according to the manufacturer's instructions. *In vitro* translated proteins were analysed by Western blotting. Experiments were repeated at least three times, and the representative results are shown.

Quantitative real-time RT-PCR. 293T cells were transfected with various expression plasmids, and harvested 24 h later. Levels of Vpx/Vpr mRNA in transfected cells were determined by quantitative real-time RT-PCR. After washes with PBS, total RNA was extracted with an RNeasy Plus Mini kit (Qiagen), and cDNA was synthesized using SuperScript III (Invitrogen) using oligo(dT) as a primer. PCR was performed with an ABI7500 (Applied Biosystems) using Power SYBR Green PCR Master Mix (Applied Biosystems). Primer sets used were: 5′-GCCAGGAAACAGTGGAGA-3′ and 5′-GCTTGGTGACATCCC-TTGGT-3′ for measurement of WT and mutant Vpx mRNAs; 5′-CTAGAGGGCCCTTCGAACAA-3′ and 5′-GCTGGCAACTAGAAG-GCACA-3′ for simultaneous measurement of Vpx and Vpr mRNAs. For normalization, a primer set specific for the human *GAPDH* gene (5′-CACCACCATGGAGAAGGCTG-3′ and 5′-GCTGATGATCTTG-AGGCTGTTGT-3′) was used. Values were calculated by the manufacturer's software. Standard curves were generated by amplifications of serially diluted cDNA samples. Experiments were repeated three times, and the mean values with standard deviations are presented.

Phylogenetic analysis. Phylogenetic analysis was performed for Vpx proteins of HIV-2/SIVs and Vpr proteins of the SIVagm group. PPM-minus SIVsyk Vpr was used as a reference. These amino acid sequences were obtained from the HIV sequence database at Los Alamos National Laboratory (http://www.hiv.lanl.gov) and aligned by the CLUSTAL_X 2.0.11 program (Jeanmougin *et al.*, 1998; Thompson *et al.*, 1997). Phylogenetic tree was generated by the neighbour-joining method using the CLUSTAL_X 2.0.11 program. The branch significance was analysed by bootstrap with 1000 replicates. The tree was visualized by the TreeView 1.6.6 program (Page, 1996) and the reference was manually removed.

ACKNOWLEDGEMENTS

We thank Ms Kazuko Yoshida for editorial assistance. This work was supported in part by the Japan Society for the Promotion of Science via a Grant-in-Aid for Young Scientists (B) to Y. M. (ID no. 24790443).

REFERENCES

Accola, M. A., Bukovsky, A. A., Jones, M. S. & Göttlinger, H. G. (1999). A conserved dileucine-containing motif in p6(gag) governs the particle association of Vpx and Vpr of simian immunodeficiency viruses SIV(mac) and SIV(agm). *J Virol* **73**, 9992–9999.

Adachi, A., Gendelman, H. E., Koenig, S., Folks, T., Willey, R., Rabson, A. & Martin, M. A. (1986). Production of acquired immunodeficiency syndrome-associated retrovirus in human and nonhuman cells transfected with an infectious molecular clone. *J Virol* **59**, 284–291.

Anraku, K., Fukuda, R., Takamune, N., Misumi, S., Okamoto, Y., Otsuka, M. & Fujita, M. (2010). Highly sensitive analysis of the interaction between HIV-1 Gag and phosphoinositide derivatives based on surface plasmon resonance. *Biochemistry* **49**, 5109–5116.

Berger, G., Durand, S., Fargier, G., Nguyen, X.-N., Cordeil, S., Bouaziz, S., Muriaux, D., Darlix, J.-L. & Cimarelli, A. (2011). APOBEC3A is a specific inhibitor of the early phases of HIV-1 infection in myeloid cells. *PLoS Pathog* **7**, e1002221.

Blanco-Melo, D., Venkatesh, S. & Bieniasz, P. D. (2012). Intrinsic cellular defenses against human immunodeficiency viruses. *Immunity* **37**, 399–411.

Doerfel, L. K., Wohlgemuth, I., Kothe, C., Peske, F., Urlaub, H. & Rodnina, M. V. (2013). EF-P is essential for rapid synthesis of proteins containing consecutive proline residues. *Science* **339**, 85–88.

Fujita, M., Otsuka, M., Miyoshi, M., Khamsri, B., Nomaguchi, M. & Adachi, A. (2008a). Vpx is critical for reverse transcription of the human immunodeficiency virus type 2 genome in macrophages. *J Virol* **82**, 7752–7756.

Fujita, M., Otsuka, M., Nomaguchi, M. & Adachi, A. (2008b). Functional region mapping of HIV-2 Vpx protein. *Microbes Infect* **10**, 1387–1392.

Fujita, M., Otsuka, M., Nomaguchi, M. & Adachi, A. (2010). Multifaceted activity of HIV Vpr/Vpx proteins: the current view of their virological functions. *Rev Med Virol* **20**, 68–76.

Goujon, C., Arfi, V., Pertel, T., Luban, J., Lienard, J., Rigal, D., Darlix, J.-L. & Cimarelli, A. (2008). Characterization of simian immunodeficiency virus SIV_{SM}/human immunodeficiency virus type 2 Vpx function in human myeloid cells. *J Virol* **82**, 12335–12345.

Gramberg, T., Sunseri, N. & Landau, N. R. (2010). Evidence for an activation domain at the amino terminus of simian immunodeficiency virus Vpx. *J Virol* **84**, 1387–1396.

Gutierrez, E., Shin, B.-S., Woolstenhulme, C. J., Kim, J.-R., Saini, P., Buskirk, A. R. & Dever, T. E. (2013). eIF5A promotes translation of polyproline motifs. *Mol Cell* **51**, 35–45.

Harris, R. S., Hultquist, J. F. & Evans, D. T. (2012). The restriction factors of human immunodeficiency virus. *J Biol Chem* **287**, 40875–40883.

Hrecka, K., Hao, C., Gierszewska, M., Swanson, S. K., Kesik-Brodacka, M., Srivastava, S., Florens, L., Washburn, M. P. & Skowronski, J. (2011). Vpx relieves inhibition of HIV-1 infection of macrophages mediated by the SAMHD1 protein. *Nature* **474**, 658–661.

Jeanmougin, F., Thompson, J. D., Gouy, M., Higgins, D. G. & Gibson, T. J. (1998). Multiple sequence alignment with CLUSTAL_X. *Trends Biochem Sci* **23**, 403–405.

Jin, L., Zhou, Y. & Ratner, L. (2001). HIV type 2 Vpx interaction with Gag and incorporation into virus-like particles. *AIDS Res Hum Retroviruses* **17**, 105–111.

Kawamura, M., Sakai, H. & Adachi, A. (1994). Human immunodeficiency virus Vpx is required for the early phase of replication in peripheral blood mononuclear cells. *Microbiol Immunol* **38**, 871–878.

Khamsri, B., Murao, F., Yoshida, A., Sakurai, A., Uchiyama, T., Shirai, H., Matsuo, Y., Fujita, M. & Adachi, A. (2006). Comparative study on the structure and cytopathogenic activity of HIV Vpr/Vpx proteins. *Microbes Infect* **8**, 10–15.

Laguette, N., Sobhian, B., Casartelli, N., Ringeard, M., Chable-Bessia, C., Ségéral, E., Yatim, A., Emiliani, S., Schwartz, O. & Benkirane, M. (2011). SAMHD1 is the dendritic- and myeloid-cell-specific HIV-1 restriction factor counteracted by Vpx. *Nature* **474**, 654–657.

Lebkowski, J. S., Clancy, S. & Calos, M. P. (1985). Simian virus 40 replication in adenovirus-transformed human cells antagonizes gene expression. *Nature* **317**, 169–171.

Mahnke, L. A., Belshan, M. & Ratner, L. (2006). Analysis of HIV-2 Vpx by modeling and insertional mutagenesis. *Virology* **348**, 165–174.

Malim, M. H. & Bieniasz, P. D. (2012). HIV restriction factors and mechanisms of evasion. *Cold Spring Harb Perspect Med* **2**, a006940.

Page, R. D. (1996). TreeView: an application to display phylogenetic trees on personal computers. *Comput Appl Biosci* **12**, 357–358.

Pancio, H. A. & Ratner, L. (1998). Human immunodeficiency virus type 2 Vpx-Gag interaction. *J Virol* **72**, 5271–5275.

Park, I.-W. & Sodroski, J. (1995). Amino acid sequence requirements for the incorporation of the Vpx protein of simian immunodeficiency virus into virion particles. *J Acquir Immune Defic Syndr Hum Retrovirol* **10**, 506–510.

Sharp, P. M., Bailes, E., Stevenson, M., Emerman, M. & Hahn, B. H. (1996). Gene acquisition in HIV and SIV. *Nature* **383**, 586–587.

Shibata, R., Kawamura, M., Sakai, H., Hayami, M., Ishimoto, A. & Adachi, A. (1991). Generation of a chimeric human and simian immunodeficiency virus infectious to monkey peripheral blood mononuclear cells. *J Virol* **65**, 3514–3520.

Singh, S. P., Lai, D., Cartas, M., Serio, D., Murali, R., Kalyanaraman, V. S. & Srinivasan, A. (2000). Epitope-tagging approach to determine the stoichiometry of the structural and nonstructural proteins in the virus particles: amount of Vpr in relation to Gag in HIV-1. *Virology* **268**, 364–371.

Thompson, J. D., Gibson, T. J., Plewniak, F., Jeanmougin, F. & Higgins, D. G. (1997). The CLUSTAL_X windows interface: flexible strategies for multiple sequence alignment aided by quality analysis tools. *Nucleic Acids Res* **25**, 4876–4882.

Ude, S., Lassak, J., Starosta, A. L., Kraxenberger, T., Wilson, D. N. & Jung, K. (2013). Translation elongation factor EF-P alleviates ribosome stalling at polyproline stretches. *Science* **339**, 82–85.

Ueno, F., Shiota, H., Miyaura, M., Yoshida, A., Sakurai, A., Tatsuki, J., Koyama, A. H., Akari, H., Adachi, A. & Fujita, M. (2003). Vpx and Vpr proteins of HIV-2 up-regulate the viral infectivity by a distinct mechanism in lymphocytic cells. *Microbes Infect* **5**, 387–395.

Zheng, Y.-H., Jeang, K.-T. & Tokunaga, K. (2012). Host restriction factors in retroviral infection: promises in virus-host interaction. *Retrovirology* **9**, 112.

ELSEVIER

Institut Pasteur

Microbes and Infection 15 (2013) 56–65

www.elsevier.com/locate/micinf

Original article

Gag-CA Q110D mutation elicits TRIM5-independent enhancement of HIV-1mt replication in macaque cells

Masako Nomaguchi [a,1], Masaru Yokoyama [b,1], Ken Kono [c], Emi E. Nakayama [c], Tatsuo Shioda [c], Akatsuki Saito [d], Hirofumi Akari [d], Yasuhiro Yasutomi [e], Tetsuro Matano [f], Hironori Sato [b], Akio Adachi [a,*]

[a] *Department of Microbiology, Institute of Health Biosciences, The University of Tokushima Graduate School, 3-18-15 Kuramoto, Tokushima 770-8503, Japan*
[b] *Laboratory of Viral Genomics, Pathogen Genomics Center, National Institute of Infectious Diseases, 4-7-1 Gakuen, Musashimurayama, Tokyo 208-0011, Japan*
[c] *Department of Viral Infections, Research Institute for Microbial Diseases, Osaka University, 3-1 Yamadaoka, Suita, Osaka 565-0871, Japan*
[d] *Center for Human Evolution Modeling Research, Primate Research Institute, Kyoto University, 41-2 Kanrin, Inuyama, Aichi 484-8506, Japan*
[e] *Tsukuba Primate Research Center, National Institute of Biomedical Innovation, Tsukuba, Ibaraki 305-0843, Japan*
[f] *AIDS Research Center, National Institute of Infectious Diseases, 1-23-1 Toyama, Shinjuku-ku, Tokyo 162-8640, Japan*

Received 5 September 2012; accepted 20 October 2012
Available online 1 November 2012

Abstract

HIV-1 is strictly adapted to humans, and cause disease-inducing persistent infection only in humans. We have generated a series of macaque-tropic HIV-1 (HIV-1mt) to establish non-human primate models for basic and clinical studies. HIV-1mt clones available to date grow poorly in macaque cells relative to SIVmac239. In this study, viral adaptive mutation in macaque cells, G114E in capsid (CA) helix 6 of HIV-1mt, that enhances viral replication was identified. Computer-assisted structural analysis predicted that another Q110D mutation in CA helix 6 would also increase viral growth potential. A new proviral construct MN4Rh-3 carrying CA-Q110D exhibited exquisitely enhanced growth property specifically in macaque cells. Susceptibility of MN4Rh-3 to macaque TRIM5α/TRIMCyp proteins was examined by their expression systems. HIV-1mt clones so far constructed already completely evaded TRIMCyp restriction, and further enhancement of TRIMCyp resistance by Q110D was not observed. In addition, Q110D did not contribute to evasion from TRIM5α restriction. However, the single-cycle infectivity of MN4Rh-3 in macaque cells was enhanced relative to the other HIV-1mt clones. Our results here indicate that CA-Q110D accelerates viral growth in macaque cells irrelevant to TRIM5 proteins restriction.

Keywords: HIV-1; HIV-1mt; Gag-CA; Macaque cells; Virus growth; Molecular modeling

1. Introduction

Mammalian cells express a variety of host restriction factors to defend themselves against pathogens. Viruses have evolved countermeasures to subvert their restriction and replicate efficiently in cells [1,2]. HIV-1, a causative agent of human AIDS, evades host restriction factors and replicates well in human cells. However, in macaques for experimental use, e.g. cynomolgus macaques (CyMs) and rhesus macaques (RhMs), HIV-1 replication is completely inhibited by host restriction factors present in their cells [3]. Construction of HIV-1 that overcomes species-barrier contributes much to understand the interaction of HIV-1 and its host as well as the establishment of HIV-1-infected macaque models [4,5].

Extensive molecular biological studies on the HIV-1/host interaction conducted to date have revealed main mechanical bases for the narrow host range exhibited by HIV-1. Macaque cells contain potent antiviral factors that effectively restrict or even abolish HIV-1 replication. These include APOBEC3 proteins (APOs), CyclophilinA (CypA), and TRIM5α/TRIMCyp

* Corresponding author. Tel.: +81 88 633 7078; fax: +81 88 633 7080.
E-mail address: adachi@basic.med.tokushima-u.ac.jp (A. Adachi).
[1] Masako Nomaguchi and Masaru Yokoyama contributed equally to this work.

1286-4579/$ - see front matter © 2012 Institut Pasteur. Published by Elsevier Masson SAS. All rights reserved.
http://dx.doi.org/10.1016/j.micinf.2012.10.013

(TRIM5 proteins). HIV-1 can indeed counteract human proteins corresponding to these restriction factors. APOs exhibit cytidine deaminase activity, and introduce lethal mutations into HIV-1 genome. HIV-1 Vif is able to neutralize the antiviral activity of human APOs, but not macaque APOs [6–8]. CypA acts on incoming HIV-1 core to regulate infection positively in human cells but negatively in macaque cells [9–11], though amino acid sequences of CypA from human and macaque are identical. Macaque TRIM5α recognizes and interacts with incoming HIV-1 core, and restricts virus infection in a less-defined mechanism [9–11]. Macaque TRIM5α is polymorphic, and has sequence variation in a C-terminal B30.2/SPRY domain important for capsid (CA) binding. Sequence variation in this domain causes modulation of host susceptibility to retrovirus infection [12,13]. Macaque TRIMCyp is a fusion protein resulted from replacement of a B30.2/SPRY domain with CypA. Both CyM and RhM cells express TRIMCyp, but affinity of these proteins to HIV-1 core is different due to amino acid substitutions in Cyp domains. Thus, CyM TRIMCyp restricts HIV-1 replication, but not RhM TRIMCyp [14,15].

Identification of host restriction factors in macaque cells and their target proteins in HIV-1 has prompted us to generate macaque-tropic HIV-1 (HIV-1mt) with a minimal modification of HIV-1 genome. We successfully constructed prototype HIV-1mt, NL-DT5R, by replacing CypA binding region on a loop between helices 4 and 5 (h4/5L) in *gag*-CA and entire *vif* genes with the corresponding regions of pathogenic SIVmac239 (Fig. 1) [16]. But growth potential of NL-DT5R was inferior to that of SIVmac239 both *in vitro* and *in vivo* [16,17]. These results indicated that genetic modifications in NL-DT5R were insufficient to confer the ability on the virus to grow efficiently in macaque cells [16–18]. In an attempt to improve growth potential of NL-DT5R, we adapted NL-DT5R and its R5-tropic version NL-DT562 to a CyM derived lymphocyte cell line HSC-F, and found a number of genetic substitutions in viral genomes of adapted viruses [19]. We introduced these mutations and CA h6/7L from SIVmac239 into NL-DT5R, and the resultant clone was designated MN4-5S (Fig. 1) [19]. MN4-5S exhibited enhanced growth potential in CyM both *in vitro* and *in vivo* compared to NL-DT5R [19]. But growth ability of MN4-5S was still lower than that of SIVmac239.

In this study, to further improve replication potential of HIV-1mt, we adapted MN4-5S in macaque cells and identified an adaptive mutation in CA that enhances growth ability in the cells. *In silico* structural modeling of the adaptive mutation predicted that Q110D mutation on helix 6 in CA (CA-Q110D) would promote viral replication in macaque cells. Indeed, a proviral clone carrying CA-Q110D, designated MN4Rh-3, exhibited marked enhancement of growth potential in macaque cells relative to all the other HIV-1mt clones we have constructed (Fig. 1). CyM TRIM5α/TRIMCyp susceptibility assays revealed that MN4Rh-3 completely evades from TRIMCyp restriction but not TRIM5α restriction as observed for the other HIV-1mt clones. While CA-Q110D contributed to neither endowment of further resistance to TRIMCyp nor evasion from TRIM5α restriction, CA-Q110D did lead to enhanced single-cycle infectivity to a macaque cell line compared with the other HIV-1mt clones. Our results here indicate that CA-Q110D accelerates viral growth in macaque cells independently of TRIM5 proteins restriction.

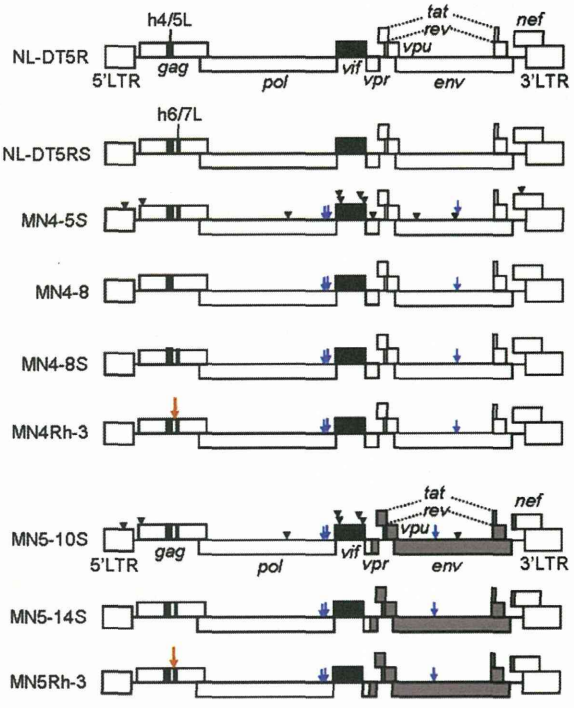

Fig. 1. Proviral genome structure of various HIV-1mt clones used in this study. HIV-1 NL4-3 [26] and SIVmac239 (GenBank: M33262) sequences are indicated by white and black areas, respectively. Gray areas in MN5-10S, MN5-14S and MN5Rh-3 show sequences from NF462 [21]. Blue arrows and black arrowheads show nucleotide substitutions that appeared in viral genomes of NL-DT5R and NL-DT562 during adaptation in HSC-F cells. Among nucleotide substitutions, adaptive mutations that enhance viral growth potential are indicated by blue arrows. Red arrows show the CA-Q110D mutation.

2. Materials and methods

2.1. Plasmid DNA

Construction of NL-DT5R, NL-DT562, NL-DT5RS, and MN4-5S were described previously [16,19–21]. MN4-5S carries all nucleotide substitutions that are present in adapted NL-DT5R and NL-DT562 clones except for mutations in the *env* gene of R5-tropic viruses (MN5-10S, MN5-14S, and MN5Rh-3 in Fig. 1) [19]. MN4-8S contains adaptive (growth-enhancing) mutations in MN4-5S but not the other mutations. MN4Rh-3 was constructed by introduction of the CA-Q110D mutation into MN4-8S. To construct R5-tropic viruses, 3′ halves of viral genomes (*Eco*RI in *vpr* to *Sph*I at the 3′ end of viral genome) of MN4-5S, MN4-8S, and MN4Rh-3 were replaced with the corresponding regions of adapted-NL-DT562,